Applied Thermal Engineering 257 (2024) 124169

Contents lists available at ScienceDirect

Applied Thermal Engineering

journal homepage: www.elsevier.com/locate/ate

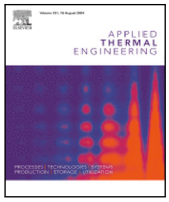

Research Paper

Solution of the modular PCM-based cooling ceiling and ventilation system

Jan Skovajsa *, Pavel Drabek, Stanislav Sehnalek

Tomas Bata University in Zlin, Faculty of Applied Informatics, Namesti T.G.Masaryka 5555, Zlin, 760 01, Czech Republic

ARTICLE INFO

Keywords:
Cooling ceiling
Energy savings
Heat accumulation
PCM
TES

ABSTRACT

Most newly constructed buildings are now built to energy-passive standards, which set requirements for specific heating demand, non-renewable primary energy use, building envelope airtightness, and the frequency of exceeding permissible indoor air temperatures in summer. These temperature exceedances relate to the room's thermal stability, determined by the potential for heat accumulation in surrounding structures over the daily cycle. For buildings with lightweight construction, implementing a Thermal Energy Storage (TES) solution can significantly enhance their energy accumulation ability. This article addresses the design and evaluation of a progressive cooling ceiling system combined with active ventilation system components, including the incorporation of TES based on PCM materials. The proposed solution aims to improve the thermal stability of occupied spaces, thereby significantly reduce the need for mechanical cooling. The research developed a new methodology for measuring the energy performance parameters of modular cooling ceiling systems, with its implementation thoroughly discussed. The evaluation of this solution was conducted within the context of the entire energy system for a reference building, considering various construction types (lightweight, medium, heavy). The overall potential energy savings range from 13% to 32%, depending on the building's construction, while still meeting the required thermal comfort criteria.

1. Introduction

The buildings and construction sector has accounted for over a third of global final energy consumption and more than a quarter of global energy-related emissions [1]. The operation of buildings alone represents a significant portion of this overall consumption. The issue of reducing the energy demand of buildings has been addressed for many years and is incorporated into various directives at the supranational level. The well-known aim of these measures is to ensure adequate indoor microclimate conditions with minimal energy input. Over the past 20 years, improvements have been made in the thermal insulation properties of building envelopes, the integration of various technological systems, optimization of their control logic, and the education of operators. As a result, since 2010, energy demand for heating has decreased by 20%, lighting by 17%, and the preparation of hot water, cooking, and other household appliances by 20%. The only area exhibiting a contrary trend is the cost of cooling buildings, which has increased by approximately 9% over this period. In general, energy consumption intensity in buildings is steadily decreasing by an average of 1% per year [1,2]. However, on a global scale, the opposite is true due to the continuous construction of new buildings driven by population growth and climate change. This imbalance led to an approximate 8% increase in energy consumption between 2010 and 2020.

Another important evaluation parameter is the quality of the indoor microclimate, which has gradually improved due to the availability of cooling and innovations in the control of individual building systems. Available data suggest that cooling is one of the main factors contributing to climate change and increasing energy consumption [1,2]. In 2020, space cooling accounted for nearly 5% of global energy demand, corresponding to approximately one gigaton of CO2 emissions. According to the International Energy Agency (IEA), energy consumption for cooling has doubled since 2000 (from 1000 TWh to 1945 TWh), mainly due to climate change, urbanization, and the increasing number of installed air conditioning units [1,2].

The aforementioned data highlight the need for research and new solutions in building cooling, focusing on efficiency, durability, operational safety, service, and other environmental and economic aspects. Support for research and development activities is also evident from manufacturers, driven by gradual legislative changes and the need to bring products to market that meet refrigerant type and energy efficiency criteria. However, this research is often addressed at the component level, focusing on the behavior of new refrigerants, optimizing individual parts of the equipment, proper sizing within the overall system, improving control logic based on system behavior under variable conditions, and utilizing new materials. Nonetheless, the

* Corresponding author.
E-mail address: jskovajsa@utb.cz (J. Skovajsa).

https://doi.org/10.1016/j.applthermaleng.2024.124169
Received 10 April 2024; Received in revised form 24 July 2024; Accepted 12 August 2024
Available online 20 August 2024

Nomenclature

A_a	Active cooling area (m^2)
P	Total cooling capacity (W)
P_a	Specific cooling capacity (Wm^{-2})
T	Temperature (K)
ΔT	Temperature Difference (K)
θ_{PCM}	Mean Phase Change Temperature of PCM (°C)
θ_{inlet}	Inlet water temperature (°C)
AC	Air Conditioning
ACH	Air Change Rate ($1 \cdot h^{-1}$)
RMSE	Root Mean Square Error (–)
RRMSE	Relative Root Mean Square Error (–)
R2	Coefficient of determination (–)
CC	Compensated Calorimetric Chamber
CEBIA-Tech	Centre for Security, Information and Advanced Technologies
CO2	Carbon Dioxide
FH	Family House
GB	Gypsum Board (Drywall)
DSC	Differential Scanning Calorimetry
SEER	Seasonal Energy Efficiency Ratio
FAI	Faculty of Applied Informatics
HRV	Heat Recovery Ventilation
HVAC	Heating, Ventilation, and Air Conditioning
PCM	Phase Change Materials
PMV	Predicted Mean Vote
PPD	Predicted Percentage of Dissatisfied
PS	Polystyrene
RC	Reinforced Concrete
TBU	Tomas Bata University
TES	Thermal Energy Storage
TRNSYS	Transient Systems Simulation Software

comprehensive evaluation of the building as a whole concerning the thermal stability of occupied zones is an issue largely unaddressed by these manufacturing entities. These matters are discussed by other professionals such as designers, integrators, installation companies, and the building services operators themselves.

Thermal comfort can be disrupted for parts of the day by external temperature fluctuations. This problem is also observed in newly constructed buildings meeting passive energy standards, particularly those made from lightweight building materials (such as timber structures), which often lack sufficient heat storage capacity. Every material can store a certain amount of heat and subsequently release it into the surroundings. This capability is critical for lightweight constructions because they cannot adequately store excess heat/cold during the daily cycle, necessitating mechanical heating/cooling to ensure thermal comfort. Higher energy consumption is thus required to eliminate temperature fluctuations in the indoor environment, especially during hot summer months. To reduce cooling demand and ensure thermal stability in rooms, it is necessary to address the utilization of excess energy and its subsequent use during periods of deficit.

A suitable approach to solving this issue is the "Avoid–Improve–Shift" concept [1]. The goal of the first part, "Avoid", is to reduce cooling energy demand through appropriate architectural and construction modifications, which are addressed during the building design phase. The "Improve" part focuses on increasing the efficiency of the cooling system and optimizing its operation in relation to other building systems. The final part,"Shift", deals with the use of renewable energy sources (RES), free cooling, and energy storage. This last part can be addressed during construction or in existing buildings. Significant progress has been made in storing electrical energy from RES into batteries, supported by the development of electromobility. Another trend is the use of large storage tanks based on the Carton battery with thermochemical and sorption reactions for energy storage [3]. These solutions, however, are intended for long-term energy storage over weeks to months. For eliminating temperature fluctuations during the day, smaller capacities can be used in the form of suitable materials integrated into buildings or cooling systems. Thermal energy storage (TES) systems are used for this purpose. TES systems provide the ability to temporarily store thermal energy in the form of heat or cold for later use, such as during periods of deficit [4]. This can cover at least part of the energy deficit typically supplied by external sources. There are three basic TES principles based on temperature change (sensible), phase change (latent), or thermochemical processes.

The latent heat accumulation method is based on the absorption or release of heat during the phase change process, which makes it advantageous due to the high accumulation energy density per unit mass [5]. Phase Change Materials (PCM) are used to accumulate thermal energy. These are important because of their ability to absorb significant amounts of latent energy during phase change, especially in the melting and solidification regions of the [6]. There are many materials with different chemical compositions, varying melting temperatures, and latent heat values. From the perspective of building and Heating, Ventilation and Air-Conditioning (HVAC) systems (range 10 °C to 60 °C), paraffin and salt hydrates are the most suitable.

The practical applications of PCM represent various possible solutions, both as part of building structures and TES systems. These can be categorized as passive and active building systems. Heier et al. [7] state that passive storage systems are charged and discharged by the temperature difference between the storage and the environment. In the case of active TES, active pumps or fans are used. There are also combinations where charging is active, and discharging is passive or vice versa.

Passive systems use the incorporation of PCMs into building components such as floors, walls, roofs, ceilings, transparent elements, and shading technology. It is also possible to integrate it in the form of plasterboards or mortar and plaster with the addition of PCM. Incorporating PCM changes the thermal-accumulation properties of building structures or parts thereof. The application of PCM can enhance the natural thermal comfort regulation by reducing temperature fluctuations [8–10], there is also a time shift and peak heat load distribution [11]. In addition, effective incorporation of PCMs can lead to more efficient operation of HVAC systems [12]. Combined PCM with waste materials, ensuring the sustainable design of energy-efficient buildings is also possible [13,14]. Passive cooling systems are particularly effective when more significant temperature differences occur.

As mentioned, the additional mechanical energy of pumps or fans is used in active cooling systems. Therefore, these systems are based on integrating the PCM with a mechanical ventilation or water system. With a suitable combination of PCM and HVAC, it is possible to achieve optimal thermal comfort as well as more efficient operation of the systems, leading to energy savings [7].

Much published research has focused on the impact of integrating PCMs into cooling systems on the dynamic behavior of the building and its process systems. This is supported by outputs from various simulation tools [11,15–18] or experiments [19–29].

Most studies show that cooling ceilings with PCM can achieve higher thermal comfort and better energy efficiency than conventional cooling systems. However, results have also shown a significant effect of climatic conditions on energy savings.

Based on the aforementioned, this article further explores the potential of using PCM in cooling systems. It presents conclusions from the entire process, from design and system analyses through measurement to evaluation and generalization of results to the active area. The

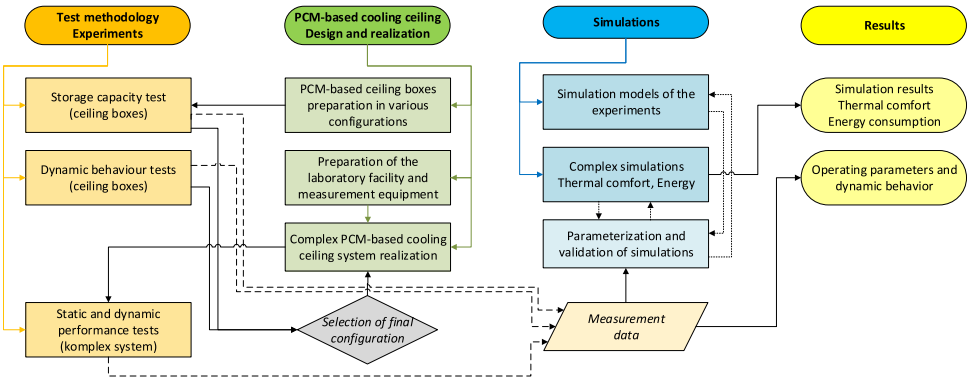

Fig. 1. Methodology - flowchart.

primary motivation for this research is the fact that available studies still lack comprehensive approaches to addressing this issue. There is a dearth of information that closely examines the impact of PCM material quantity on system efficiency throughout the day, methods for determining energy performance parameters in a laboratory setting and evaluating the solution in combination with other systems, including its impact on thermal comfort in the room. This article addresses many of these questions and can serve as a foundation for other research teams focusing on specific aspects of this problem. The article outputs are test methodologies and a modular solution utilizing both passive and active cooling system components, allowing precise control of energy flow to and from the room. Potential directions for further research and approaches to their resolution are also discussed.

2. Methodology

This research paper is generally focused on integrating phase change materials, PCMs, into selected environmental engineering systems, specifically ceiling cooling and ventilation systems. Appropriately applying accumulation materials in building structures or HVAC systems can ensure thermal stability, especially in summer and transitional parts of the year. This will also provide a higher level of thermal comfort. In addition, by using the stored energy efficiently, a reduction in the energy consumption of the building can be achieved, thus meeting global energy consumption targets in the building sector.

The presented research is extensive and complex, covering several research areas, each with additional sub-areas containing a significant volume of information and data. The main areas can be divided into Design and realization, Test methodology and Experiments, Simulations, and Results. All individual parts of the research are interconnected and directly related to each other. A schematic flowchart is presented in Fig. 1.

In the research section "Test Methodology and Experiments", entirely new laboratory measurements and test methodologies are prepared for ceiling cooling systems with additional thermal accumulation mass. The individual tests can be categorized into three main groups: Storage capacity test, Dynamic behavior tests of the system's components, and Static and dynamic performance tests of the overall system.

Simultaneously, a design proposal is prepared, followed by the preparation of various configurations of prototype ceiling thermal storage boxes. These boxes are subsequently subjected to storage capacity and dynamic behavior tests. A suitable configuration for a modular ceiling cooling and ventilation system is selected based on the acquired data. Once the comprehensive system is ready, it undergoes static and dynamic performance tests.

In parallel with the methodology and prototype preparation, simulation models corresponding to the conducted experiments and comprehensive models are developed to assess the impact on thermal comfort and energy consumption. All data obtained from measurements are used for parameterization and validation of the prepared simulation models. Once the simulation models are verified, comprehensive simulations describing real-world applications could be conducted.

The final stages of the research involve processing and evaluating the measured and simulated data to determine operational parameters, dynamic behavior, impact on thermal comfort, and energy consumption across various configurations and applications.

In the following sections of the article will be described:

- Introduction of the laboratory facilities, measuring equipment, and used PCM.
- Technical design and implementation of individual elements and complex ceiling cooling system with energy storage.
- Preparation of methodologies for laboratory experiments.
- Performing experiments and determining actual operating parameters.
- Preparation and parameterization of complex simulation models.
- Determination of the effect of the application on thermal comfort and energy consumption in the building.

2.1. The laboratory facilities and measuring equipment

The practical part of the work was carried out in the Laboratory of Environmental Engineering (LEE), part of the regional research center CEBIA-Tech at Tomas Bata University, Faculty of Applied Informatics (FAI TBU) in Zlin. The central part of the LEE is a universal compensated calorimetric chamber (CC), designed as a two-layer construction with compensation for the influence of the surrounding environment. The CC contains two reconditioning spaces, Indoor (IDO) and Outdoor (ODO), with one shared calibrated, multi-purpose partition. Both spaces are additionally surrounded by their own compensation space. The internal dimensions of the Indoor space are 4.0 × 4.3 × 3.3 m, and the Outdoor space is 8.0 × 4.3 × 3.3 m. The overall external dimensions of the chamber are 13.8 × 5.8 × 4.8 m. A view of the outer envelope and a section through the 3D CC model can be seen in Fig. 2.

Different microclimatic conditions can be maintained in CC test spaces. IDO part has the operating air temperature range from +5 °C to +60 °C, and ODO from −25 °C to +50 °C. The required dry and wet bulb values, or relative humidity, for the different types of tests, are specified in the relevant standards. A precisely controlled heat exchanger station is available for working fluid preparation and is connected to the reconditioning unit's cooling and heating circuits.

In CC, it is possible to measure the parameters of various devices such as air-conditioners, air-to-air and air-to-water heat pumps, chilled ceilings and beams, induction or fan units, distribution elements, etc. In addition, it is possible to determine the acoustic parameters of various devices and materials. As simulators of the human body, load dummies can also be deployed in the test space. Due to the available possibilities

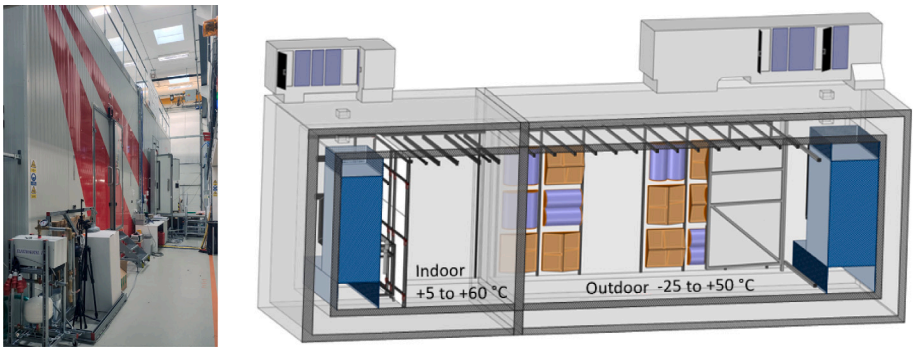

Fig. 2. Shell and half 3D model of the compensated calorimetric chamber.

and capacities CC represents, these were used to perform the individual experiments.

However, the experiments could only be started after proper preparations of the IDO space, e.g.: preparation of the hydraulic connection of the ceiling cooling system and construction of the tight partition. After these preparations, the IDO space will be divided into a test and a source section. The test section has a floor area of 10.75 m^2 and a height of 3 m after modification. The next point was to ensure the required emissivity of ≥ 0.9 of the internal surfaces. Finally, the room was equipped with continuously adjustable load dummies, the power and number determined by the requirements of standard EN 14240.

As part of the preparation of the laboratory facilities, it was necessary to provide, among other things, the necessary measuring equipment. List of instruments and measuring devices used:

- Almemo 2690, Almemo 86909A and Almemo 500.
- Humidity temperature probe Rotronic HC2A-S (RV±0.8%, T±0.1 K).
- Pt100 Greisinger GTF101P temperature sensors (1/10 DIN class B).
- Almemo ZA9020-FS type K thermocouples (±0.1 K, calibrated with calibration bath Lauda ECO RE 1050 S).
- Almemo FPA686 foil temperature sensor (Pt100 DIN class B).
- Ball thermometer Almemo FPA805GTS (inside Pt100 DIN class B).
- Almemo FQA018C heat flux sensors (±5%).
- Almemo FVAD05TOK300 thermo-anemometric omnidirectional sensors (±3% of measured value +1% of range (0.050 to 2.500 m/s)).
- Magnetic-induction flowmeter KROHNE OPTIFLUX2000 (±0.5%).
- AirFlow PTSXR-K micromanometer (±1.25 Pa).
- Electrical measurement module B&R X20AP3131 (±1.8%).

Examples of the CC preparation are captured in Fig. 3 below.

2.2. PCM DuPont Energain

DuPont's product PCM Energain was used in the research. This material comes in the form of 5.26 mm thick panels (PCM 5 mm and aluminum packaging 2 × 130 μm). The panel filling is a molecularly encapsulated paraffin wax and ethylene polymer mixture. Due to the encapsulation method, the mixture has no liquefaction even when the phases change, and the panels can be freely cut and split [30,31]. The disadvantage of organic PCMs is that they are flammable in nature. The chosen PCM Energain has a flash point of 148 °C, which can be considered safe for the low and medium temperature applications considered, i.e., 10 °C to 40 °C.

The selected PCM was subjected to differential scanning calorimetry (DSC) with a heating rate of 0.5 K min^{-1}, see Fig. 4.

The data shows a range of melting and solidification temperatures between 18 °C and 24 °C. This range is suitable for applications in passive systems, providing thermal comfort, and active systems, e.g., for space cooling. The PCM Energain is able to accumulate more than 100 kJ kg^{-1} over this temperature range. To give an idea, Table 1 shows a comparison with equivalent volumes or masses of common building materials.

Table 1
Equivalent volumes and weights with the same storage capacity.

Material	Volume [m^3]	Weight [kg]
PCM DuPont Energain	1	1
Isover Woodsil	481	20.8
Ytong	21.9	16.7
Porotherm	18,6	17,4
Concrete	6,4	16,3
Iron	4.1	37.9
Water	3.4	4.0

2.3. Design and realization of the PCM-based cooling ceiling prototype

The proposed system is based on a combination of PCM-based cooling ceiling boxes and a chilled beam. The ceiling boxes act as a passive storage element with the possibility of external heating and cooling. The chilled beam is then an active ventilation element. In addition, the entire system is hydraulically interconnected to allow appropriate control of the energy flows in the different parts of the system.

The technical design dealt with the structural design of the individual parts of the proposed system. The schematic in Fig. 5 shows a section of a 1.4 × 0.8 × 0.2 m storage chilled ceiling box made of 1.5 mm thick sheet metal with a matt white finish. This box was then filled with several layers of PCM Energain. A tubular heat exchanger is placed between them.

Ceiling boxes should be prepared in four different configurations: 2-2-0, 2-2-1, 2-2-2, and 2-2-3, where the first and last values represent the number of layers below and above the heat exchanger, the middle two layers form the fill between the heat exchanger pipes. The construction is designed so that the heat exchanger is a fully integrated part of the storage core of the boxes.

The used chilled beam (Trox DID632-LR-2-M/1200x593x210) is equipped with a finned heat exchanger, which can be blown by air flow, both circulating and fresh. Fig. 6 shows a section and a 3D image of the beam.

In the final version, the system is connected to a hydraulic circuit consisting of ceiling boxes, a chilled beam, a circulation pump, and a plate exchanger for active heating and cooling of the heat transfer medium, see Fig. 7.

The principle of the circuit implies the possibility of independent activation of ceiling boxes and beams in combination with natural or mechanical ventilation. Generally, the system modes can be listed as:

Fig. 3. Preparation of the measuring area in the IDO part of CC.

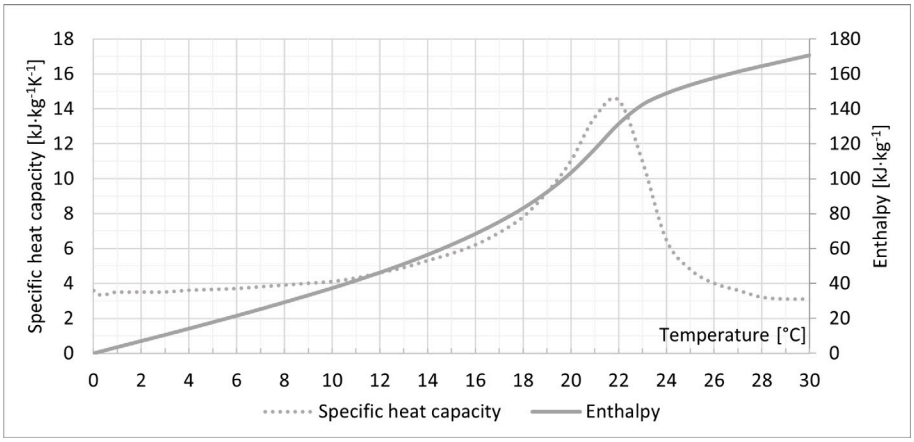

Fig. 4. DSC curve for PCM Energain.

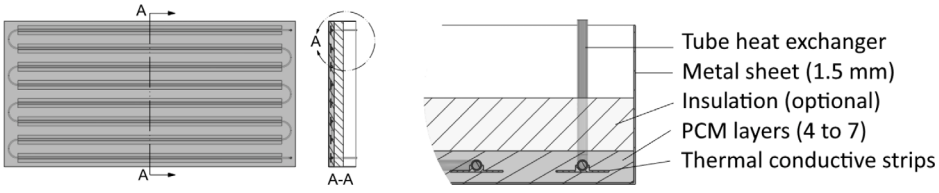

Fig. 5. Composition of the ceiling cooling box.

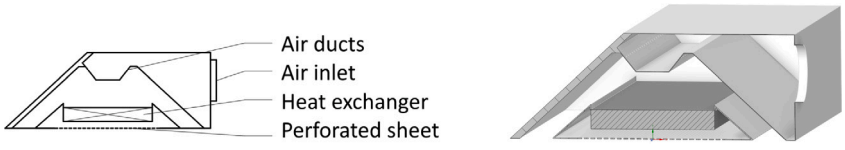

Fig. 6. Section and a 3D image of the chilled beam.

passive without circulation of the heat transfer medium; semi-active without external cooling and heating; active with external cooling or heating; the former in combination with non-/active airflow through the beam.

The passive mode is a typical application of PCM materials, i.e., it can reduce temperature peaks and stabilize the temperature in the monitored area during the day and night. It can be used to increase the efficiency of passive (night) cooling.

The semi-active mode, without external cooling and heating, uses the circulation of the heat transfer medium within the ceiling boxes and the beam exchanger, which offers an additional heat transfer surface that can be supplemented by forced convection. This mode can also be used in combination with free cooling.

Active mode with external sources is used when the storage capacity of the PCM is exhausted, or there is an immediate requirement for a temperature change in the room. In this mode, it is possible to use the chilled beam's maximum power while accumulating cold in the PCM boxes for later use.

The implementation of the ceiling cooling prototype is based on the technical design. The procedure consisted of several steps: providing sheet metal boxes with the required dimensions and surface finish, a water exchanger in aluminum rails, and a sufficient number of PCM

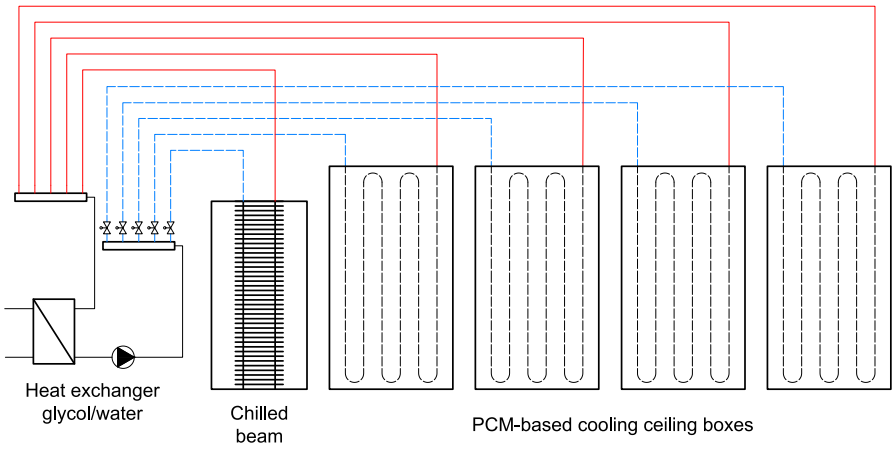

Fig. 7. Hydraulic connection of the ceiling cooling/heating system.

Fig. 8. Detail of PCM panel and ceiling box with heat exchanger.

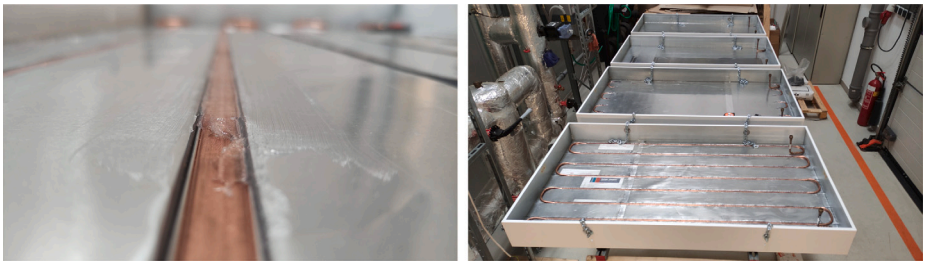

Fig. 9. Filling gaps with fused PCM and prepared configurations.

panels. The Fig. 8 shows the detail of the PCM panel cut and the prepared box with the heat exchanger.

All the boxes were filled with two layers of PCM according to the configurations considered. The next step was to insert the water exchanger, which was glued to ensure sufficient contact with the PCM. Once the heat exchanger was in place, the space between the pipes needed to be filled. Here, it was necessary to prepare two layers of precisely shaped strips of PCM that would fit as snugly as possible and be in direct contact with the heat exchanger.

It was necessary to fill all the gaps with molten PCM to ensure direct contact between the heat exchanger and the PCM, see Fig. 9 on the left. This ensured the best possible contact with the heat exchanger and mutual coupling of the PCM. This completed the configuration 2-2-0. The following procedure was to insert additional layers of PCM above the heat exchanger, thus finishing the 2-2-1, 2-2-2, and 2-2-3 configurations, see Fig. 9.

Calculations were simultaneously performed for the expected parameters when designing individual variants of ceiling accumulation boxes. These parameters include the amount of PCM used, accumulation capacity, time constant, and cooling power. The theoretical cooling power is derived from the heat transfer coefficient, which depends on the geometric composition of the boxes (pipe spacing, PCM thickness above and below the heat exchanger), the chosen PCM properties, and the heat transfer coefficient from the fluid to the pipes and from the surface to the surroundings. The heat transfer coefficient to the surroundings was determined by natural convection and radiation calculations. The calculations accounted for conditions involving a horizontally positioned plate heated from both above and below.

Table 2
Expected parameters.

PCM layer composition	[pcs]	**2-2-0**	**2-2-1**	**2-2-2**	**2-2-3**
Total weight of PCM	[kg]	18.2	23.2	28.1	33.1
Accumulation capacity	[kJ]	3 107	3 674	4 241	4 808
Time constant	[h]	3.4	4.6	5.9	7.6
Specific capacity	[Wm^{-2}]	97	87	84	76

The anticipated parameters for each variant of the ceiling boxes are presented in Table 2.

The average values of the PCM parameters in the temperature range 0 °C to 30 °C, and the mean effective temperature differences $\Delta T = 10$ K were used in considered calculations.

As can be seen from the expected parameters, the composition and number of PCM layers have an effect on the storage capacity and

fundamentally affect dynamic behavior and specific cooling performance. More layers increase the storage capacity and the time constant but also reduce the specific cooling capacity. This is due to the fact that the individual layers represent the thermal resistance between the exchanger and the surface of the box.

2.4. Test methodology - experiments

Considering the complexity of the problem concerning thermal energy storage, it was necessary to prepare procedures for partial experiments that are able to capture aspects and parameters of systems with heat accumulation. The first step was to determine the accumulation capacity of the different configurations of the prepared boxes. Then, placing the ceiling boxes in the ODO part of the CC was possible. The individual configurations' dynamic processes, including the environment's influence, were tested there. Finally, a complete active ceiling cooling and ventilation system was installed in the IDO part of the CC, where it was subjected to static and dynamic tests to determine realistic parameters under different operation modes.

2.4.1. Measuring the storage capacity of ceiling boxes

The methodology consists of controlled cyclic charging and discharging (heating and cooling) of the ceiling boxes without any influence from the surrounding environment. This test can be carried out both inside and outside the CC. However, the essential requirement is to achieve the best possible thermal insulation of the ceiling boxes to prevent losses to the surroundings.

Boundary conditions: inlet water temperature, θ_{inlet}, should be set and maintained at $\theta_{\text{inlet}} = \theta_{\text{PCM}} \pm \Delta T$, where θ_{PCM} corresponds to the assumed mean phase change temperature and the working temperature difference $\Delta T = 8$ to 10 K. The water flow rate is not defined, but ensuring a sufficient temperature difference between the inlet and the outlet is recommended, i.e., to choose a lower flow rate.

From the measured data, it is possible to determine the accumulation capacity of the individual configurations. At the same time, cyclic charging and discharging ensure that the potential hysteresis occurring in the PCM in the melting and solidification region is captured throughout the process. A snapshot of the measurements can be seen in Fig. 10 on the left.

2.4.2. Measuring dynamic behavior with environmental effects

The methodology consists of monitoring the course of parameters of individual ceiling box configurations under variable conditions of the water circuit or the surrounding environment. Four measurements can be made in these tests: active heating/cooling by varying the inlet water temperature and passive heating/cooling by varying the ambient temperature.

Boundary conditions: inlet water temperature, $\theta_{\text{inlet}} = \theta_{\text{PCM}} \pm \Delta T$, where θ_{PCM} corresponds to the assumed mean phase change temperature and the working temperature difference $\Delta T = 8$ to 10 K. The water flow rate should ideally be set to the design value, i.e., the one that should also be used in the performance tests, see chapter 2.4.3. The ambient temperature is given by the expected limiting conditions, i.e., about 14 °C to 16 °C in cold conditions mode and about 26 °C to 28 °C in warm conditions. During testing, ensure that the lowest surface temperatures of the cooling ceilings and hot water piping are above the dew point temperature of the ambient air.

These measurements must be made where the required parameters of the water circuit and the surrounding environment can be independently adjusted and maintained. In this case, the ODO part of the CC was used, where the connection to the heat exchanger station (supply from IDO) and the active adjusting of the ambient air parameters was available. The preparation of the boxes in the Outdoor part of CC can be seen in Fig. 10 on the right.

2.4.3. Performance measurement of ceiling cooling system

The methodology is based on the procedures specified in the technical standards EN 14240, EN 14518, and EN 15116, which deal with measuring the cooling capacity of chilled ceilings and beams. The proposed ceiling cooling system with heat storage in combination with an active beam cannot only be tested according to these standards, which monitor performance parameters under steady-state conditions, but the methodologies needed to be adapted and extended to include procedures that cover dynamic changes, mainly, cooling capacity ramp-up and ramp-down under different conditions.

Boundary conditions: During individual tests, the specified temperature difference $\Delta T = T \pm 1$ K is used, where $T = \{6; 8; 10\}$ K. The temperature difference ΔT is given by the difference between the reference air temperature (measured with a globe thermometer) and the mean cooling water temperature [32]. The reference air temperature should be maintained between 22 °C and 27 °C. During the measurement, it is necessary to ensure minimum heat loss through the surrounding walls; for this reason, the temperature in the surrounding compensation space is kept at the same temperature as the temperature inside the measured space. During the tests, it is also necessary to ensure that the inlet temperature of the coolant is at least 2 K higher than the dew point temperature of the ambient air. The manufacturer may determine the water flow rate according to the expected performance, or a reference value shall be established, which will result in a temperature difference between the inlet and outlet of 2 K at an operative temperature difference of 8 K.

Measurements can only be made in a space that meets the requirements of the standards, which define the dimensions of the space, the parameters of the materials used, the installation of ceiling elements, the emissivity of surfaces, and the location and parameters of load dummies to balance the cooling performance. The measurements were carried out in the prepared measurement space of the IDO part of the CC, see Fig. 11, which complies with the requirements of the standards.

The individual tests can determine the total and specific cooling capacity at standard conditions in different operating modes, from passive to fully active. It is also possible to observe the ramp-up and ramp-down of the system's cooling capacity with constant or variable heat load in various operation modes.

2.5. Simulation

The presented research contained many partial simulations and experimental procedures that have been suitably combined. The aim was to achieve the implementation of a cooling ceiling system with PCM and to determine the overall impact of its applications on energy consumption and thermal comfort.

The research mainly used the simulation software TRNSYS, which can be used to analyze and simulate thermal processes in buildings, energy flows, electricity consumption, etc. The prerequisites for achieving relevant and further usable results are suitably selected input data, especially parameters of the area of interest, structures, and climatic conditions.

First, simulation models corresponding to the proposed experiments were created and parameterized. These models were validated with experimental results to verify the correct parameterization of the model parts. Once adequate quality was achieved, the validated modules could be used in more complex simulations.

The final part of the simulation procedures was the design and preparation of complex simulations that included the applications of the designed cooling ceiling and ventilation system under conditions corresponding to the real environment. These simulations address various building structures, space utilization, air change rates, active cooling area ratios, and operating modes. From the obtained data, it is possible to determine the influence of the variable parameters on the final energy consumption for cooling or heating and the operative

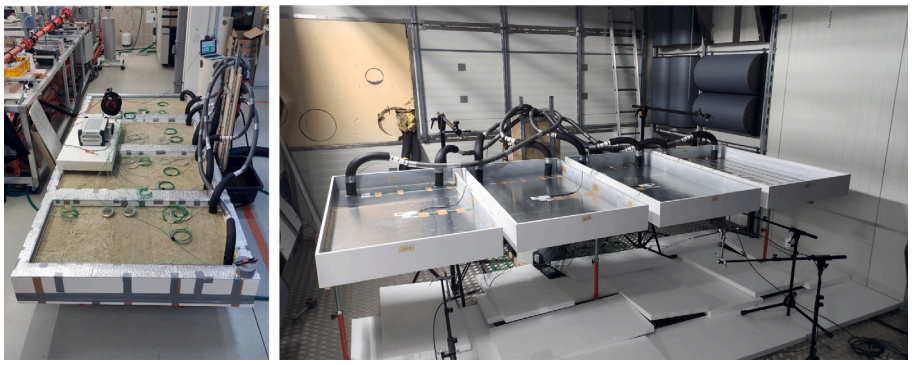

Fig. 10. Measurements of storage capacity and dynamic processes.

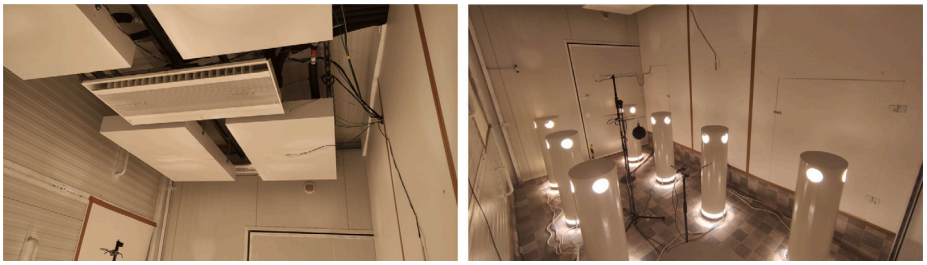

Fig. 11. Measurement of ceiling cooling system in IDO part of CC.

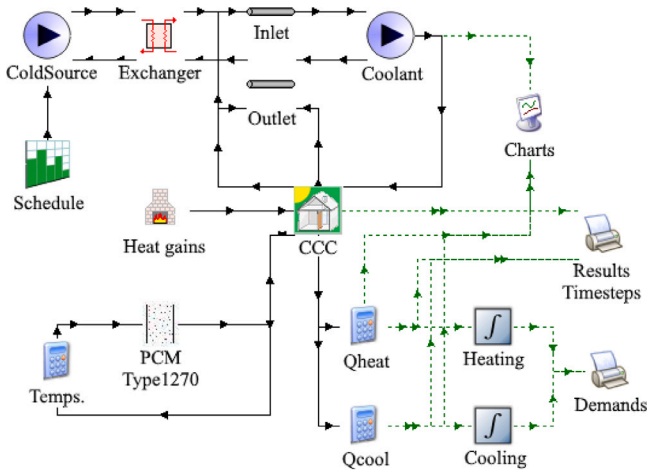

Fig. 12. Schema of the computational model - experiment.

temperature, as well as the thermal comfort indicators Predicted Mean Vote (PMV) and Predicted Percentage of Dissatisfied (PPD).

The PMV value expresses the mean thermal sensation of a group of people in a given environment. It can be determined by a subjective assessment of the thermal sensation of people using a seven-point scale (+3 is hot, 0 is neutral, and −3 is cold) or by calculation according to EN ISO 7730 [33]. The primary input data for the calculation are the metabolic rate, thermal resistance of clothing, air temperature, mean radiant temperature, relative humidity, and air velocity.

The PPD value then predicts the percentage of people dissatisfied with the environment. Its value can be determined by calculation if the PMV is known:

$$PPD = 100 - 95\exp(-(0,03353 \cdot PMV^4 - 0,2179 \cdot PMV^2)). \quad (1)$$

The calculation shows that it is not possible to satisfy all persons. The lowest PPD value can be 5%, assuming the PMV is 0.

Table 3
Simulation quality indicators.

Parameter	RMSE [± unit]	RRMSE [%]	R^2 [–]
Operative temperature	± 0.104 °C	0.4	0.956
Inlet water temperature	± 0.134 °C	0.8	0.999
Outlet water temperature	± 0.138 °C	0.8	0.998
Surface temperature	± 0.180 °C	0.8	0.995
Heat load/cooling capacity	± 5.467 W	4.8	0.999
External power supply	± 13.287 W	2.8	0.998

2.5.1. Simulation models of the experiments

The simulation models of the experiments were modeled in TRNSYS software using Multi-Zone Building (Type56) modules with necessary components such as PCM module (Type1270), pumps, piping, heat exchanger, time and control functions, and others (plotters, equations, integration, etc.), see Fig. 12.

The Type56 module representing the CC was set up as a space free from the influence of the external environment and equipped with an active cooling ceiling with PCM. The parameterization of the cooling ceiling was made according to the real tested system, and the settings of each component were adjusted according to the corresponding experiments, such as air temperature, flow rates, heat exchanger and piping parameters, internal heat load, and operation schedule. These simulation models were then compared with the results of the experiments performed in CC.

The quality of the simulations can be determined using indicators such as the Root Mean Square Error RMSE, the Relative RMSE (RRMSE), and the coefficient of determination R^2. More accurate simulations have lower RMSE or RRMSE, and further, the higher the value of R^2, the better the model fits the measured data set. In terms of optimization and validation of simulation and experimental results, the most critical parameters are the operative temperature, the surface temperature of the cooling ceiling, the heat load (cooling capacity), the inlet/outlet water temperature, and the water flow rate. Table 3 gives the qualitative simulation indicators for the selected parameters.

The calculated values of the quality indicators show a high level of agreement between simulated and measured data. Thus, such a tuned

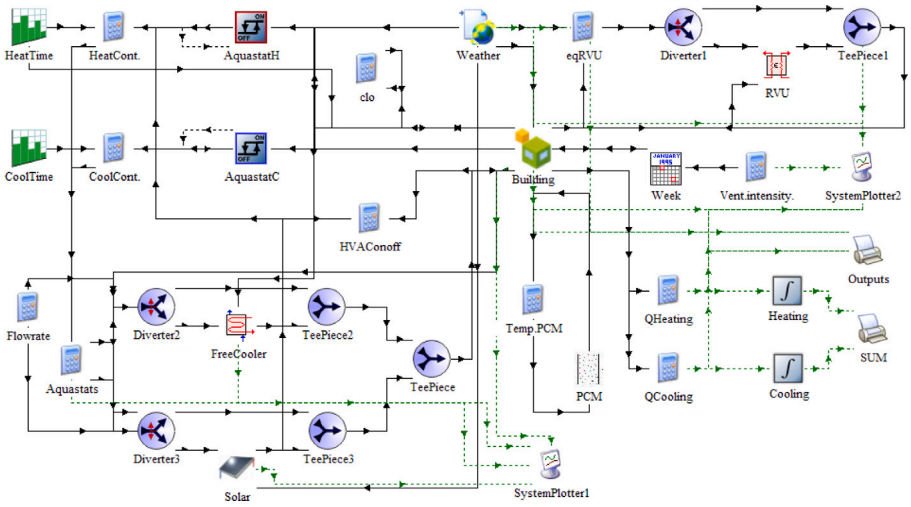

Fig. 13. Schema of the complex simulation model.

and validated PCM-based cooling ceiling system model can be used in complex simulations with sufficient accuracy.

2.5.2. Complex simulations

The comprehensive simulation model uses the Multi-Zone Building module as a base with additional modules such as the PCM module, pumps, heat exchangers, heat recovery, controllers, schedules, control functions, and more (calculations, conversions, numerical and graphical outputs), see Fig. 13. The weather profile was obtained from the weather station at FAI TBU in Zlín (Czech Republic, Central Europe, average values from 2017 to 2021). The weather dataset contains, among others, values of location, dry bulb temperature, relative humidity, atmospheric pressure, solar radiation, wind direction, and wind speed.

The reference space models were parameterized using TRNBuild. In this interface, it is possible to define and parameterize in detail all design elements and system settings of the HVAC. It is also possible to prepare arbitrary occupancy plans, air change rates, internal gains, etc.

Four sets of complex simulation models were prepared for different spaces: the living room in a family house (FH) and a large office. In addition, the room in the FH was designed considering different building structures, specifically lightweight (timber frame), medium (Ytong), and heavyweight (Porotherm) structures.

Each set includes simulation models for a reference space with a conventional HVAC system and the proposed system. The aim is to observe the PCM application's effect and consider combinations of different active cooling ceiling area ratios, air change rates (ACH), and operating modes. The complete set finally contains dozens of simulation models with different settings of the required parameters.

The room simulation model in FH was set up with the following parameters:

- Dimensions: 5 × 4 × 2.7 m.
- Cover exposed from two sides of the world (south and east).
- South facing window, total 4 m^2.
- Shading of window panels, shading factor 0.5.
- Heat recovery ventilation unit (HRV) with 75% efficiency.
- Heat source: electric boiler.
- Source of cooling: air conditioner (5.1 SEER).
- Air change intensity (ACH): 0.5 h^{-1} to 2.0 h^{-1}.
- Cooling ceiling system with PCM, active area ratio 30% to 75%.
- Air temperature max. 26 °C in summer and min. 20 °C in winter.

As already mentioned, the FH simulation models were prepared for different building structures that share the above parameters but differ in the composition of the envelope and internal structures.

As the first type of building structure, a wooden building was selected whose external walls have the following composition: gypsum board (GB) (15 mm), partition with mineral wool (40 mm), GB with a vapor barrier (13 mm), frame with mineral wool (120 mm), GB (15 mm), thermal insulation (160 mm) and facade system. The envelope thus constructed has an area weight of approximately 95 kg m^{-2} and therefore falls into the lightweight construction category [34]. Internal partition composition: GB (15 mm), frame with mineral wool (60 mm), and GB (15 mm). Composition of the ceiling under the unheated attic: GB (15 mm), ceiling structure filled with mineral wool (180 mm), chipboard (22 mm), and thermal insulation (100 mm). Floor: reinforced concrete slab, polystyrene (PS) (160 mm) and floor covering.

The second selected type is masonry construction using the Ytong system. The composition of the external walls: internal plaster (7 mm), Ytong standard (300 mm), thermal insulation (150 mm), and exterior plaster (8 mm). The area weight is approximately 140 kg m^{-2} and thus also falls into the heavy construction category but is considered medium-weight within the research scope. Composition of internal partitions: Ytong (125 mm) with double-sided plaster (7 mm). The ceiling and floor constructions are identical to the previous type.

The third type is a brick building using Porotherm cut bricks. The composition of the external walls: internal plaster (10 mm), Porotherm 44 Eko+ Profi (440 mm), thermal insulation (80 mm), and a facade system. The area weight of the above structure is approximately 320 kg m^{-2}, which puts it in the heavy construction category. Composition of internal partitions: Porotherm 11,5 Profi (115 mm) with double-sided plaster (15 mm). The ceiling and floor construction are identical to the previous types.

All of the above types of building structures are in designs that have almost identical heat transfer coefficients and, at the same time, meet the requirements for recommended values according to CSN 73 0540-2 [34].

Occupancy schedules and internal heat gains were implemented as a daily profile. The total heat flux from users, appliances, and lighting is shown in Table 4.

The last type of construction is a large office made of reinforced concrete skeleton. The composition of the external walls is considered: internal plaster (10 mm), thermal insulation (100 mm), reinforced concrete (RC) (150 mm), thermal insulation (200 mm), and facade system. The area weight of the above structure is approximately 380 kg m^{-2}, which puts it in the heavy construction category. Composition of internal partitions: Porotherm 11,5 Profi (115 mm) with double-sided plaster (15 mm). Ceiling structure: suspended ceiling

Table 4
Total heat flow rate from occupants, appliances, and lighting - FH.

Time From–To	Total heat flow [Wm^{-2}]
7:00–17:00	8.0
17:00–23:00	20.0
23:00–7:00	2.0
Average	9.0

Table 5
Total heat flow rate - office.

Time	Total heat flow [Wm^{-2}]		Time	Total heat flow [Wm^{-2}]	
From–To	Mon–Fri	Sat,Sun	From–To	Mon–Fri	Sat,Sun
0:00–7:00	0.0	0.0	13:00–14:00	13.8	0.0
7:00–8:00	4.6	0.0	14:00–16:00	16.1	0.0
8:00–10:00	13.8	0.0	16:00–17:00	13.8	0.0
10:00–12:00	16.1	0.0	17:00–18:00	4.6	0.0
12:00–13:00	9.2	0.0	18:00–0:00	0.0	0.0

Table 6
Experimentally determined heat capacity parameters.

PCM layer composition	[pcs]	**2-2-0**	**2-2-1**	**2-2-2**	**2-2-3**
Total weight	[kg]	50.7	56.4	62.2	67.3
Accumulation capacity	[kJ]	2 906	3 597	4 294	4 860
Accumulation capacity	[Wh]	807	999	1 193	1 350
Specific acc. capacity	[kJ m^{-2}]	2 624	3 248	3 877	4 388

(100 mm), RC (200 mm), thermal insulation (260 mm), and waterproofing (2 mm). Floor above the heated space: floor structure (70 mm), floor PS (30 mm), RC (150 mm), and suspended ceiling (100 mm).

The simulation model was prepared with the following parameters:

- Dimensions: 8 × 14 × 3 m.
- Corner office facing south and east.
- Window fillings total 46 m^2.
- External shading of window panels, shading factor 0.5.
- Heat recovery ventilation unit (HRV) with 75% efficiency.
- Central heat source.
- Air conditioning cooling (5.1 SEER).
- Air change intensity (ACH): 0.5 h^{-1} to 2.0 h^{-1}.
- Ceiling cooling system with PCM, active area ratio 30% to 75%.
- Air temperature max. 26 °C in summer and min. 20 °C in winter.
- Maximum occupancy: 10 m^2 per person, i.e. 11 person.
- Total load from persons: 11 Wm^{-2}.
- Total load from appliances and lighting: 12 Wm^{-2}.

The daily occupancy profiles for determining the internal heat gains from users, appliances, and lighting were determined in accordance with EN ISO 52016-1 and EN 16798-1 [35,36]. Table 5 shows the total heat flux.

3. Results and discussion

3.1. Experimental measurements of ceiling boxes and the whole system

The first experiment was to determine the storage capacity of the individual ceiling box configurations. Cyclic charging and discharging were used to minimize the influence of the surrounding environment according to Section 2.4.1. The measured values are given in Table 6.

During the measurements, the heating and cooling behavior was observed to be different over the range of phase change temperatures, i.e., 18 °C to 24 °C. It was found that the cooling of the PCM from 30 °C to 18 °C is, on average, 25% faster than the heating from 12 °C to 24 °C. In any case, the overall heating process (from 12 °C to 30 °C) is up to 40% faster than the complete cooling. This is due to the gradual change of phases with different thermal conductivity coefficient values in the liquid and solid states.

Subsequently, dynamic tests were carried out under variable inlet water conditions or the surrounding environment. First, active water cooling and passive reverse air heating were tested under stable ambient conditions. The ambient air temperature was set and maintained during the test at 27 °C. The ceiling boxes were allowed to stabilize at the ambient air temperature, and then the phase of active water cooling was started. The inlet water temperature was set and maintained at the desired value of 12 °C. Once all configurations reached stable conditions, the passive heating phase was initiated by shutting down active cooling (switching off the pump and the cooling source). The cooled ceiling boxes were naturally heated using ambient air. The test was completed after the temperatures returned to the initial conditions.

The Fig. 14 represents the course of the cooling performance in active and passive mode. On the x-axis is the achieved percentage of maximum cooling capacity (from 130 Wm^{-2} for 2-2-0 to 118 Wm^{-2} for 2-2-3). On the y-axis is a heating and cooling time. In the case of active water cooling, the cooling capacity increases from 0% to 100%; on the contrary, in the case of passive air heating, the cooling capacity decreases from 100% to 0%, i.e., from right to left.

The results show that within an hour, each configuration can achieve 65% to 80% of its maximum performance with active water cooling. On the other hand, reverse passive heating shows that the 2-2-2 and 2-2-3 configurations still have around 57% of performance after 6 h, while the 2-2-1 and 2-2-0 versions are already below 50% and 20%, respectively.

The next test was active water heating and reverse passive cooling. The process of active heating and passive cooling was similar to the previous one. The test was started by reaching initial conditions where the ambient air and cooling boxes temperatures were equal to 15 °C. The active water heating was started with an inlet water temperature of 30 °C. After reaching stable conditions, the active heating was stopped (switching off the pump and the heat source), thus starting the phase of passive cooling. The heated ceiling boxes were allowed to cool naturally with the ambient air. The test was completed after the temperatures returned to the initial conditions.

Fig. 15 shows the heating capacity course, similar to the previous test. In this case, on the x-axis is the achieved percentage of maximum heating capacity (from 144 Wm^{-2} for 2-2-0 to 116 Wm^{-2} for 2-2-3).

In this test, the individual configurations are able to reach about 40% to 70% of maximum capacity within an hour. With passive cooling, a rapid discharge is visible, with the 2-2-2 and 2-2-3 configurations having about 30% of power after 6 h and the 2-2-1 and 2-2-0 versions having under 27% and 21%.

Observing different rates of active and passive phases is possible. These differences are influenced by the construction of the boxes and the varying thermal conductivity of the PCM. In the case of active cooling, a faster initial power increase can be observed because the PCM begins to solidify near the heat exchanger, increasing thermal conductivity towards the box surface. Conversely, the PCM gradually melts during active heating, reducing thermal conductivity. The situation differs in the region of maximum performance due to the box's design, as the inner space is more effectively aired out by natural convection. For passive phases, a similar situation can be observed. The initial part of passive heating for a smoothed box exposed to ambient air is slower because the PCM gradually melts from the surface inward, decreasing thermal conductivity. In contrast, the process is slightly faster for passive cooling with molten PCM due to its gradual solidification. Measurements also reveal that the onset of PCM phase change is only sometimes apparent, occurring gradually within the box core. Once the PCM changes phase, there is a noticeable shift in performance behavior, as the process occurs primarily in the region of significant heat accumulation.

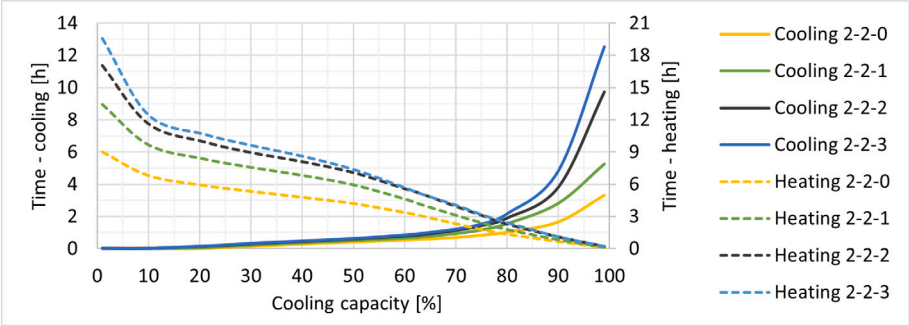

Fig. 14. Active cooling and passive heating - course of performance.

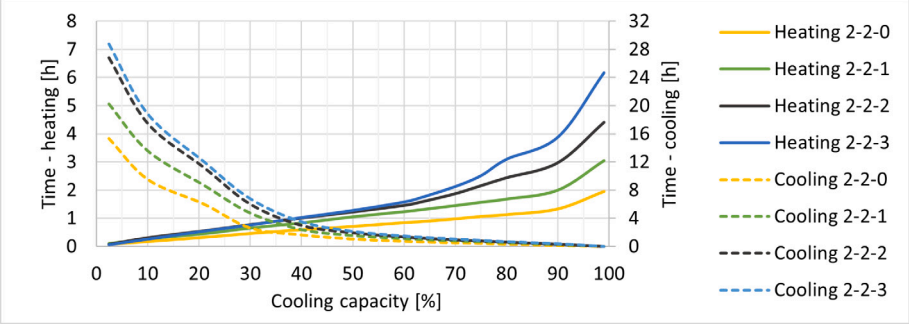

Fig. 15. Active heating and passive cooling - course of performance.

Table 7
Normalized cooling capacity for $\Delta\theta = 8$ K.

		Mode1	Mode2	Mode3
$P_a = k \cdot \Delta\theta^n$	Total capacity P [W]	301	340	713
	Specific capacity P_a [Wm^{-2}]	73.5	83.0	174.3
	Coefficient k [–]	10.951	12.037	37.188
	Exponent n [–]	0.916	0.929	0.743

In the context of ceiling cooling research, it is essential that individual boxes have consistent cooling performance over an extended period or accumulate cooling for later utilization.

Based on the results, the 2-2-2 configuration was selected for further testing. So, the following tests and results are valid for a complex system consisting of four 2-2-2 ceiling boxes with a total capacity of approximately 4.8 kWh.

The next set of tests measured the system's total and specific cooling capacity according to Section 2.4.3. These were carried out for three operating modes: ceiling boxes only (mode 1), boxes and passive chilled beam (mode 2), and fully active (mode 3) (see Table 7).

The proposed modular system can achieve promising specific cooling capacity values based on the results. Even the ceiling panels, without ventilation, can reach 73 Wm^{-2} to 83 Wm^{-2} specific cooling capacities. These values are comparable to conventional water-cooled systems, which achieve normalized values around 56 Wm^{-2} in a closed configuration and approximately 90 Wm^{-2} to 100 Wm^{-2} in an open configuration [37].

In recent studies on ceiling cooling with PCM integration can be found, Gallardo and Berardi achieved a performance of approximately 25 Wm^{-2} to 40 Wm^{-2} [26], Kang et al. reported 54 Wm^{-2} to 58 Wm^{-2} [27], Mousavi et al. reached up to 8.5 $Wm^{-2}K^{-1}$ [28], respectively 68 Wm^{-2} for a normalized temperature difference of 8 K, and Andrés-Chicote et al. achieved up to Wm^{-2} [29].

The final set of tests involved testing the system's performance ramp-up and ramp-down. These tests were performed to determine the effect of the additional thermal-accumulation mass.

The first test was an active ramp-up and passive ramp-down test with a variable heat load, i.e., constant air temperature. This test represents a situation where there is an immediate demand for space cooling and a subsequent ramp-down of the cooling performance when the heat gains of the space are gradually decreasing. The progress of the parameters is plotted in Fig. 16. As can be seen, with active cooling, 75% of the maximum cooling capacity was reached after one hour and over 90% after 3 h. A steady state was reached after less than 8 h. In the case of passive ramp-down, the progress was gradual without significant fluctuations. After 3 h, the cooling performance was still around 75%; after 7 h, it was around 50%, and the complete discharge of the cold occurred after about 20 h. During the ramp-down phase, the system absorbed around 3.3 kWh of thermal energy.

Secondly, the passive ramp-down and active ramp-up performance tests were carried out with a constant heat load, i.e., with variable air temperature. During the test, it was observed how long the air temperature was to rise by 3 K and then return to initial conditions. The progress of the test can be seen in Fig. 17. A temperature increase of 3 K occurred after about 8 h, with a decrease in cooling capacity of about 37%. During this part, the system absorbed around 2.9 kWh of thermal energy. After reactivation of the water cooling, there was a rapid increase in cooling capacity and, after a while, also a drop in temperature. After 2 h of cooling, 95% power was achieved, and the temperature dropped to 26 °C. The return to initial conditions took 10 h.

The third test was similar to the previous one, with the only difference being that when the temperature was raised by 1 K, after about 3.5 h, the water circulation in the system was turned on, including the chilled beam circuit. This led to removing cold from the boxes and increased the cooling performance using the passive mode of the chilled beam (air circulation turned off). The limiting temperature increase of 3 K occurred after about 10 h. Reverse cooling then took less than 11 h. Complete cold exhaustion was achieved in less than 9 h. During this part, the system absorbed around 3.2 kWh of thermal energy. The progress of the test is shown in Fig. 18.

Last, the ramp-down performance test from fully active mode (including air circulation 43 m^3h^{-1}) was carried out. The progress is

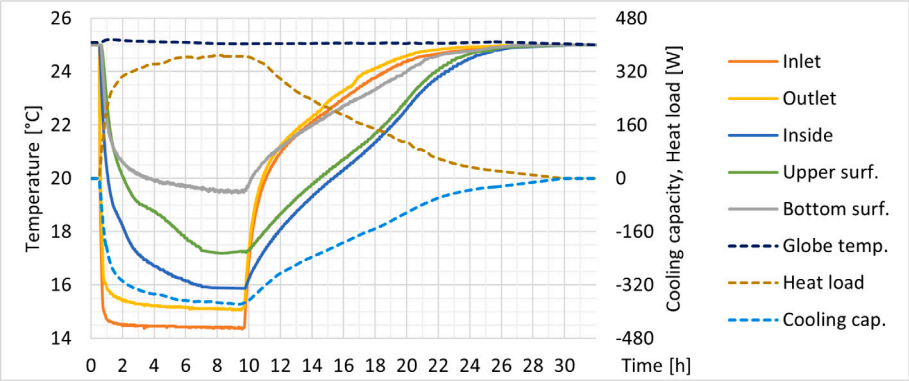

Fig. 16. Ramp-up and ramp-down; ceiling boxes; variable heat load.

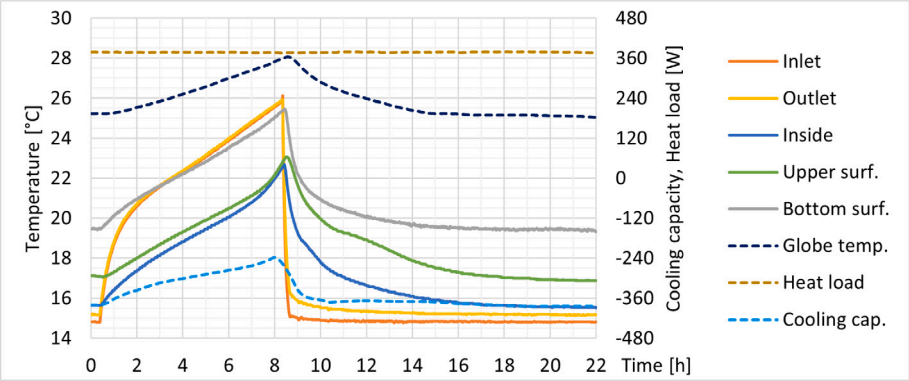

Fig. 17. Ramp-down and ramp-up; ceiling boxes; constant heat load.

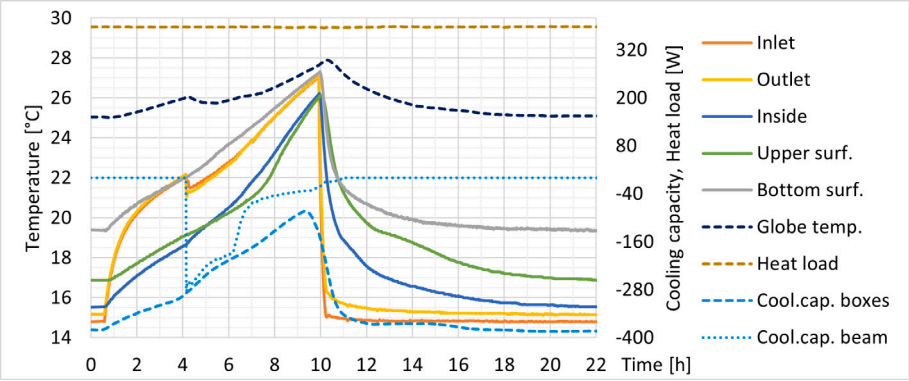

Fig. 18. Ramp-down and ramp-up; ceiling boxes with beam; constant heat load.

shown in Fig. 19. After about 2 h, the cooling power was around 420 W, i.e., 50% of the maximum power; after 5 h, it was about 20%. Like in the first test, the system absorbed approximately 3.3 kWh of thermal energy. In this case, the influence of the controlled flow of energy, including the active beam, is monitored when the effort is to ensure the rapid use of stored energy, e.g., in case of a temporary high demand for cooling.

It is evident from the available data that the proposed system can gradually transfer the stored thermal energy to the surrounding environment and, if necessary, ensure the relatively quick availability of cooling power.

It should be noted that the tests consider the expected temperatures of the real environment and applications. On the other hand, these are test procedures to help determine the dynamic behavior of the cooling ceiling systems containing storage mass. Once unified procedures are used, it will be possible to compare different systems and their configurations.

From the conducted literature review, it is evident that the application of PCMs in building environments offers significant potential for both energy and long-term financial savings. Published studies demonstrate the integration of PCM materials into transparent structures, into external walls with energy flow management using capillaries, into floor heating systems combined with PV systems, and, as in our case, directly into HVAC systems. However, the performance parameters of these various solutions cannot be directly compared, as the evaluations are specific to the particular application and boundary conditions. For this reason, we consider the proposed methodology for evaluating different large-area systems with additional accumulation material to be highly beneficial.

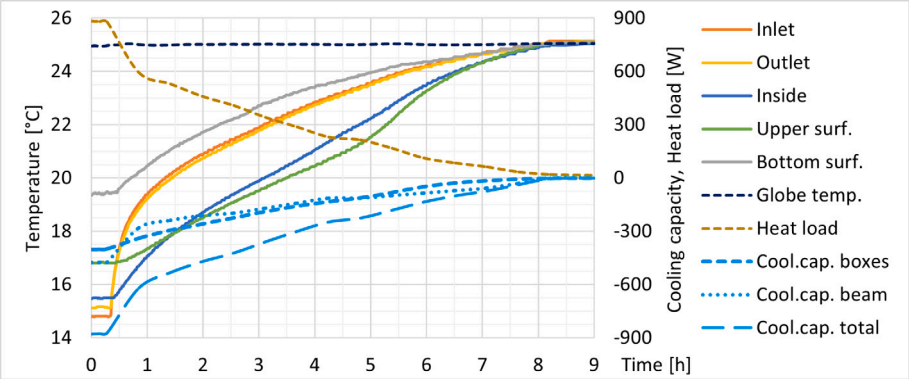

Fig. 19. Ramp-down from fully active mode; variable heat load.

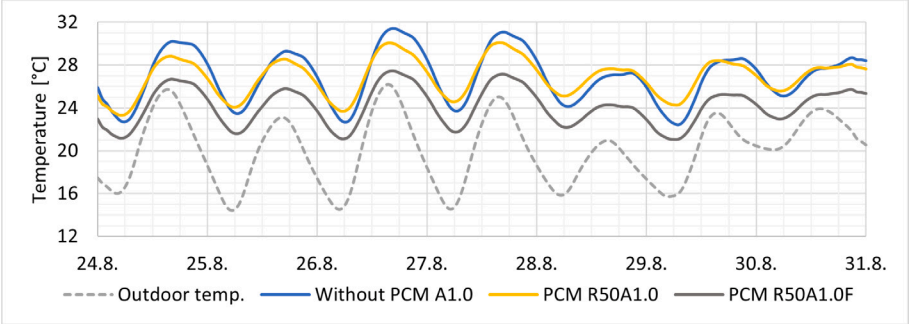

Fig. 20. Operative temperature - lightweight design.

3.2. Simulations - results

First, simulation models corresponding to the experiments were prepared. Parameterization and adjustment of the models were carried out until the corresponding results were successfully validated with real data from the measurements.

The main objective was to prepare complex simulations that include applications of the designed ceiling cooling and ventilation system in conditions corresponding to the real environment.

As mentioned, four sets of complex simulation models were prepared for different spaces: the living room in FH and the large office. For the FH, the issue of varying building structures, which are light (Wood), medium (Ytong), and heavy (Porotherm), was addressed. Furthermore, different air change rate (ACH) values, active cooling area ratios, and operating modes were addressed in these simulations.

In the following section of the article, abbreviations define the individual parameters of the ceiling cooling system with PCM application. The complete abbreviation is RxxACF, where Rxx is the active cooling area ratio (xx - percent), AC indicates if an external cooling source is used, and F indicates if free cooling is used. Examples: R30 - passive mode, active area ratio 30%; R50F – semi-active mode using free cooling, ratio 50%; R75ACF – fully active mode with external cooling source, ratio 75%.

From the extracted results of the complex simulations, the effect of the application of the designed cooling system on thermal comfort and energy consumption was subsequently determined.

3.2.1. Thermal comfort

The thermal comfort of the indoor environment is mainly defined by the operative temperature or the PMV and PPD indices. The Fig. 20 compares the operative temperature courses of the reference space of the lightweight FH construction and the space with the applied cooling ceiling system in passive and semi-active mode (with free cooling; without mechanical cooling) for illustrative purposes.

The graphs in Fig. 21 represent the determined maximum operating temperatures. These values were obtained for various building structures, different configurations of ceiling cooling, and air exchange intensities. For each structure, temperatures are depicted for the reference space without cooling (Ref.), with mechanical cooling (Ref. AC), and the space supplemented with the proposed PCM-based cooling and ventilation system. The designed system considers different active surface areas, and it operates in passive mode (Rxx) and semi-active mode (RxxF) without utilizing an external cooling source or mechanical cooling.

In passive mode, it is possible to achieve a reduction in temperature peaks of up to 2.2 °C for light-weight construction, 1.9 °C for moderately heavy construction, 2.2 °C for heavy construction, and up to 2.7 °C for office spaces. In semi-active mode, using free cooling and controlled energy flow, temperature peaks can be eliminated by up to 6.2 °C for light-weight construction, 6.1 °C for medium-weight construction, 5.6 °C for heavy-weight construction, and up to 5.6 °C for office spaces.

As mentioned before, one of the indicators of thermal comfort is the Predicted Percentage of Dissatisfied (PPD) index, representing the percentage of users dissatisfied with indoor environment conditions. The graphs in Fig. 22 depict the average seven-day PPD values for different construction types.

As can be seen, even the passive mode positively impacts thermal comfort, reducing PPD for all FH construction types by approximately 3% to 6% and for offices by 2% to 6%. In the semi-active mode, the influence is more significant, and in almost all configurations, the resulting PPD value is below 10%, approaching its minimum value of 5%. In this operational mode, it is possible to achieve a reduction in PPD (compared to Ref. AC) for light-weight and medium-weight constructions by approximately 5% to 36%, for heavy-weight by 4% to 23%, and for offices by 3% to 8%.

From these results, it is possible to infer, among other things, which configuration of the proposed system in each mode can achieve or even

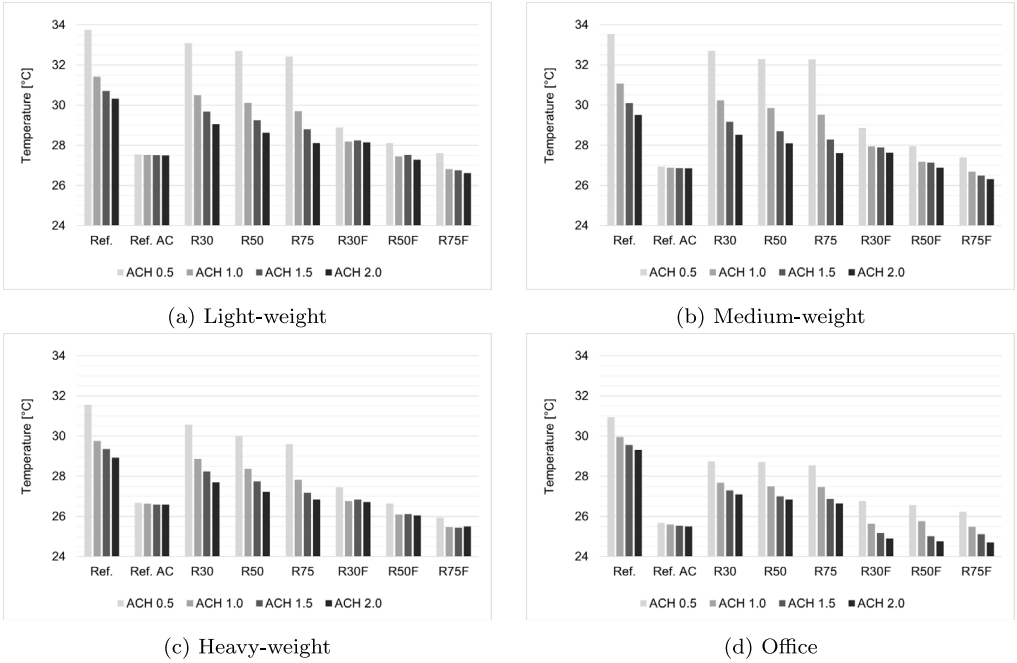

(a) Light-weight (b) Medium-weight

(c) Heavy-weight (d) Office

Fig. 21. Maximum operative temperatures.

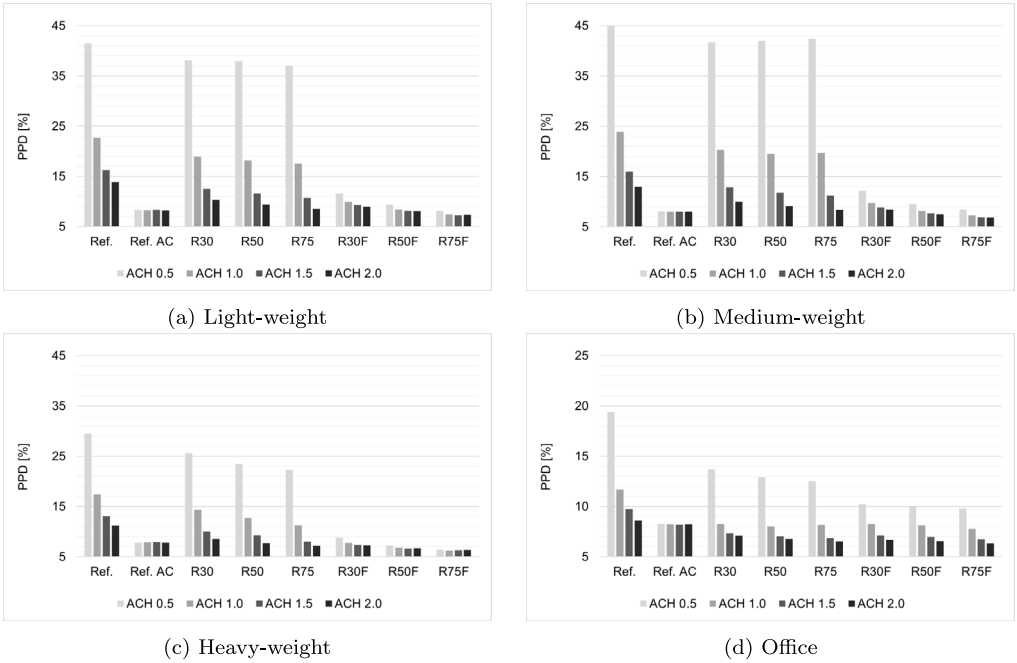

(a) Light-weight (b) Medium-weight

(c) Heavy-weight (d) Office

Fig. 22. Average PPD values.

surpass the thermal comfort values in an environment where standard ceiling cooling is used. For FH with light and medium-weight constructions and the ACH value of 1.0 h^{-1}, the sufficient configuration would be R50F. The R30F would suffice for heavy-weight FH construction, as the reference thermal comfort is already at a higher level due to the substantial thermal storage capacity of the construction. Similarly, in the case of offices, configurations R30F or R50F are suitable.

The results indicate that improving thermal comfort can be achieved by increasing the ACH. Additionally, thermal comfort continues to improve with larger active surface areas of the ceiling cooling system at each ACH value.

In all observed cases, the proposed system can provide higher thermal comfort. In passive mode, this primarily involves eliminating temperature peaks. Once a semi-active mode is available, allowing complete control of the system and leveraging the full potential of phase change material (PCM), comparable or even higher thermal comfort can be achieved compared to conventional mechanical cooling. Furthermore, neither operational mode utilizes an additional cooling source.

For clarity, the following figures represent only one selected level of ACH 1.0 h^{-1}. At the same time, values for the designed structures and different active area ratios (R30% to R75%) are plotted.

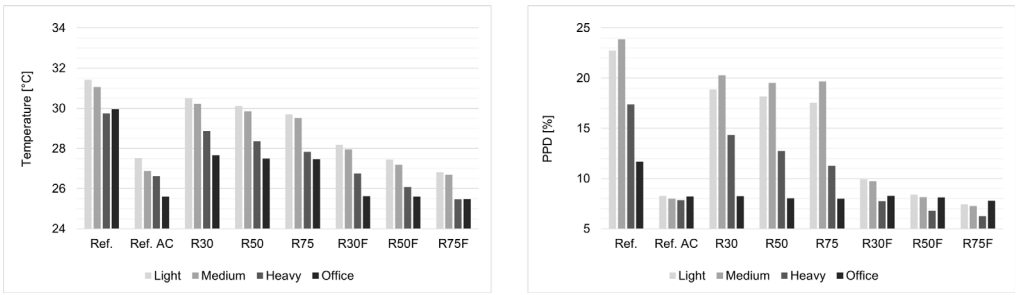

Fig. 23. Summary results for ACH 1.0 h^{-1}.

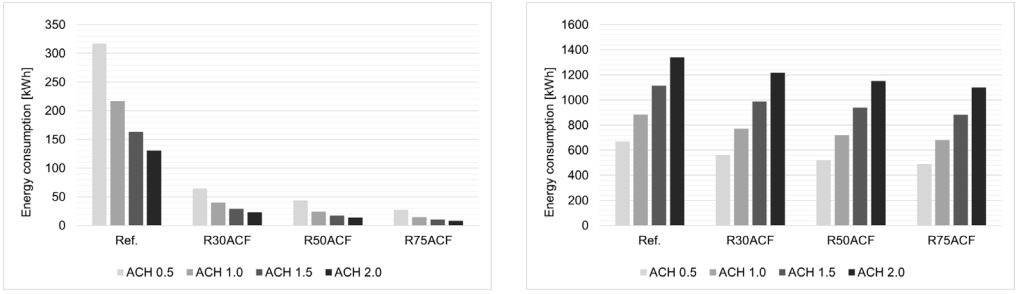

(a) Cooling (b) Heating

Fig. 24. Annual energy consumption - cooling and heating, light-weight.

The values of the maximum operative temperatures and PPD values are shown in Fig. 23. As can be seen, for the FH at a given ACH, a reduction in temperature peaks of 0.8 °C to 1.8 °C on average, was achieved in passive mode, or 2.9 °C to 4.5 °C in the case of semi-active mode. So, in neither case is machine cooling used. For the office space, the reductions were around 2.5 °C and 4.5 °C. In the case of PPD, the passive mode reduced PPD values within units of percent. However, a significant improvement could be achieved in the semi-active mode. As was mentioned before, the configurations R50F (for the light/medium-weight FH design) and R30F (for the heavy-weight FH and office space) would be sufficient to achieve a similar or better effect than standard machine cooling.

3.2.2. *Energy savings*

Applications of the designed ceiling cooling and ventilation system in various configurations were also investigated from the point of view of energy consumption. The primary assignment of the system is to reduce energy consumption for space cooling. However, its application also affects heating.

It should be noted that the addressed spaces are equipped with a recuperative ventilation unit with an estimated efficiency of 75% and external shading elements, which ensures a significant reduction in consumption already in the reference state of the space. Thanks to this, the results are closer to real applications where these modern systems are increasingly installed. It is also worth mentioning that the results are presented in the form of final consumption, i.e., in the case of cooling, the energy requirement is divided by the SEER factor, see chapter 2.5.2.

Fig. 24 presents the detailed results for the light-weight structure. The effect of the active area and the ACH value on the resulting energy consumption for cooling and heating was observed. As can be seen, increasing the ACH value results in a reduction in cooling energy consumption but, at the same time, increases heating requirements. On the other hand, installing the proposed system and increasing its active area reduces final consumption in any case.

The Figs. 25 and 26 present the annual energy consumption and savings for cooling and heating of space with an ACH value of 1.0 h^{-1}. It is clear from the data that the largest relative savings were achieved in space cooling. Reductions up to 98% were achieved for FH and 81% for office. From the results related to thermal comfort, suitable ratios of active area were identified. Specifically, the optimal value for light and medium-weight constructions is R50, while for heavy-weight constructions and office spaces, it is advisable to use R30. In these cases, savings of approximately 90% for FH spaces and 70% for office space can be achieved.

In the context of heating, which is not the primary function of the proposed system, it is also possible to achieve significant savings. In particular, this is a feature of the additional storage mass in the space. From the results, it was found that reducing heat consumption by up to 23% for FH and 15% for office were achieved. Suppose the selected ratio of the active area is taken into account. In that case, savings of approximately 16% to 18% are achieved for medium and light-weight FH and about 12% for heavy-weight FH and office.

In real building use, the aim is to reduce the energy consumption. In winter, it can be practically ensured by reducing ventilation losses, i.e., by lowering the ACH value. Regarding the summer period, it is possible to reduce the cooling energy demand most of the time by increasing the ACH. This may be contrary to the requirements of standards and regulations regarding air change standards and generating pollutants, especially in winter. However, the reality is that, in both FH and offices, there is often a preference for reducing energy demand over normative requirements.

The Fig. 27 represents the total real energy savings. The resulting values are relative to the cases where the ACH is increased to 2.0 h^{-1} in summer and decreased to 0.5 h^{-1} in winter.

From the results, it is possible to determine that with a lightweight structure, it is possible to achieve a total saving of the final energy consumption of 221 kWh to 326 kWh, i.e., 22% to 32%. Similar results can be achieved for a medium-weight construction, with savings ranging between 189 kWh and 279 kWh, i.e. 21% to 30%. For heavy construction, the values are further reduced from 168 kWh to 237 kWh, corresponding to a saving of 17% to 24%. For an office space, the total savings range from 1 043 kWh to 1 246 kWh, corresponding to only 13% to 16%.

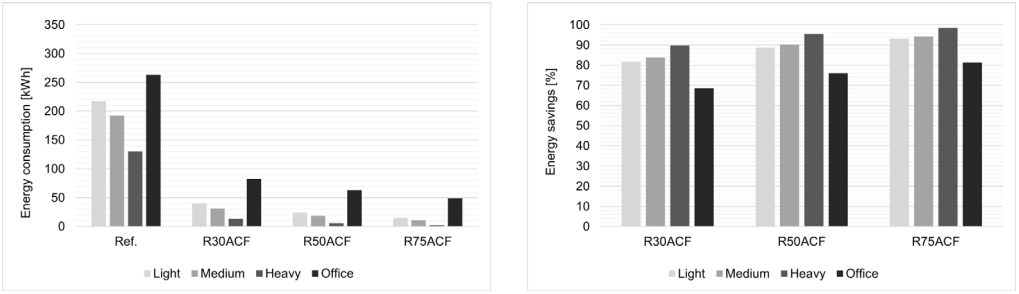

Fig. 25. Annual energy consumption and savings - cooling.

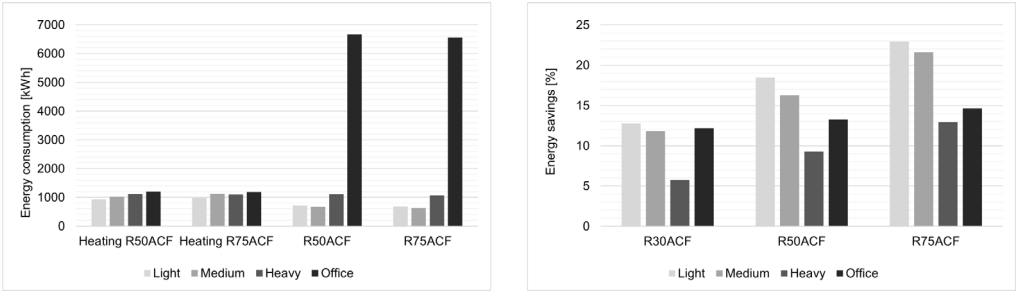

Fig. 26. Annual energy consumption and savings - heating.

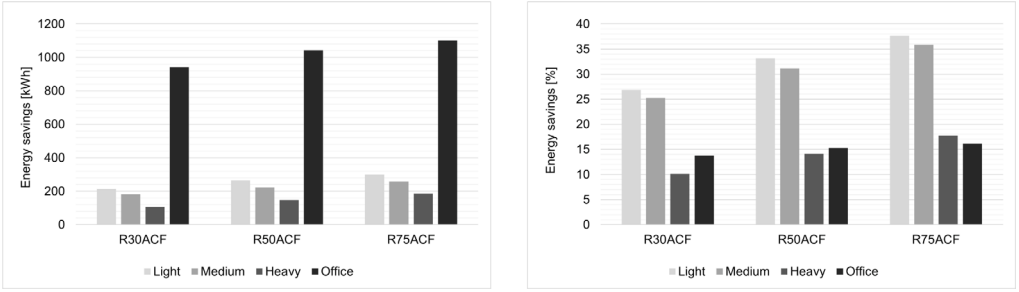

Fig. 27. Total energy savings - overview.

If the selected ratio of the active area is considered, the overall savings are 28/25/17% for light/medium/heavy-weight construction and 13% for office space. The most significant savings are achieved in lighter structures with insufficient storage capacity.

An important fact is that if it were possible to temporarily exceed the air temperature limit, i.e., 26 °C, it would be possible to eliminate the operation of mechanical cooling, especially for FH. With an appropriate design and use of the potential of the presented system, considerable financial savings can be achieved either by having a lower capacity of mechanical cooling or it will not be installed at all.

The presented solution utilizes more efficient energy flow control, including managed utilization of PCM's storage capacity, unlike similar PCM-based cooling systems. The proposed modular system combines the benefits of passive systems, TES elements, and active components for air conditioning. This solution brings sufficient cooling capacity, increased thermal comfort, and reduced energy consumption. Other research articles state that energy savings from 5% to 25%, in some cases over 30% depending on the boundary conditions and specified time-period [38,39]. It is necessary to emphasize that the lack of approaches for determining the performance parameters of PCM-based cooling ceiling systems and that available articles are focused on specific conditions (construction types, climate conditions, regime, etc.) are manifested here. So, it is challenging to compare the research results. Every application is different and cannot be categorized; on the other hand, it should be possible to use comparisons based on standardized laboratory methodologies under specific conditions.

4. Conclusion

This article presented a comprehensive research effort focused on the design and evaluation of a modular solution encompassing both passive and active components for precise energy flow control, including TES solutions based on PCM. The primary objective was to enhance the thermal comfort of occupied spaces and reduce reliance on mechanical cooling systems. The study discussed the design of a prototype modular ceiling cooling system, developing a measurement methodology for cooling systems with additional thermal accumulation mass, and evaluating the benefits of the proposed solution in buildings with various construction compositions (light, medium, heavy). Results were obtained both from a performance perspective for individual system components and from the standpoint of the overall complex modular solution, considering the dynamic behavior of the entire building. Integrating passive ceiling cooling and active ventilation systems allows for precise thermal flow control, fulfilling thermal comfort criteria.

Key findings include:

- New recommended test methodologies are presented based on existing standards and the laboratory's experience.
- A specific accumulation capacity of 2.36 MJ m^{-2} was achieved for the chosen ceiling box configuration.
- A cooling capacity of up to 83 Wm^{-2} without ventilation was achieved.

- With an active area ratio of 30% to 50%, the semi-active mode can provide the same or higher thermal comfort than conventional AC.
- The application of the tested system has a significant effect on thermal comfort. In passive mode, it was possible to eliminate temperature peaks by up to 2.7 °C and up to 6.2 °C in the case of semi-active mode. In these cases, the average PPD value was reduced by 6% to 36%.
- The most significant potential energy savings is for space cooling - up to 90% savings for family house constructions and 70% for office space.
- Overall energy savings range from 13% to 32%, depending on the building's construction type.

The presented results indicate a significant potential of the proposed solution in terms of energy efficiency, which could lead to the complete elimination of the need for mechanical cooling within the context of the building's thermal energy storage capacity. Overall, the research offers a comprehensive and insightful approach to addressing buildings' thermal comfort and energy efficiency issues, laying the groundwork for further advancements in this field.

Future research may focus on the design of large-area passive radiant ceiling systems to improve heat transfer from the cooling medium to the interior space. Currently, these systems are most often implemented into suspended ceilings, creating a separate space from the living area. The goal will be to find solutions with an open ceiling structure combined with appropriate HVAC outlet designs to meet the requirements for air exchange intensity. Comparison of these solutions will primarily be conducted on a virtual model using Computational Fluid Dynamics (CFD) simulation methods.

Declaration of competing interest

The authors declare that they have no known competing financial interests or personal relationships that could have appeared to influence the work reported in this paper.

Data availability

Data will be made available on request.

Acknowledgments

This work was supported by the European Regional Development Fund under the project CEBIA-Tech Instrumentation No. CZ.1.05/2.1.00/19.0376 and by the Ministry of Education, Youth and Sports of the Czech Republic within the National Sustainability Programme project No. LO1303 (MSMT-7778/2014) and also by the project INTERREG V-A SK-CZ/2019/11 No. NFP304010Y280.

References

[1] 2021 Global Status Report for Buildings and Construction: Towards a Zero-emissions, Efficient and Resilient Buildings and Construction Sector, Global Alliance for Buildings and Construction, International Energy Agency and the United Nations Environment Programme, 2021.
[2] Tracking buildings 2021, 2021, URL https://www.iea.org/reports/tracking-buildings-2021.
[3] R. Tiskatine, A. Aharoune, L. Bouirden, A. Ihlal, Identification of suitable storage materials for solar thermal power plant using selection methodology, Appl. Therm. Eng. 117 (2017) 591–608, http://dx.doi.org/10.1016/j.applthermaleng.2017.01.107, URL https://www.sciencedirect.com/science/article/pii/S1359431116324383.
[4] D.N. Nkwetta, F. Haghighat, Thermal energy storage with phase change material—A state-of-the art review, Sustainable Cities Soc. 10 (2014) 87–100, http://dx.doi.org/10.1016/j.scs.2013.05.007.
[5] S. Ali, S. Deshmukh, An overview: Applications of thermal energy storage using phase change materials, Mater. Today: Proc. 26 (2020) 1231–1237, http://dx.doi.org/10.1016/j.matpr.2020.02.247, 10th International Conference of Materials Processing and Characterization.
[6] S. Ali, S. Deshmukh, An overview: Applications of thermal energy storage using phase change materials, Mater. Today: Proc. (2020) http://dx.doi.org/10.1016/j.matpr.2020.02.247.
[7] J. Heier, C. Bales, V. Martin, Combining thermal energy storage with buildings – a review, Renew. Sustain. Energy Rev. 42 (2015) 1305–1325, http://dx.doi.org/10.1016/j.rser.2014.11.031, URL https://www.sciencedirect.com/science/article/pii/S1364032114009629.
[8] M. Song, F. Niu, N. Mao, Y. Hu, S. Deng, Review on building energy performance improvement using phase change materials, Energy Build. 158 (2018) 776–793, http://dx.doi.org/10.1016/j.enbuild.2017.10.066, URL https://www.sciencedirect.com/science/article/pii/S037877881732916X.
[9] B. Jelle, S. Kalnæs, Chapter 3 - phase change materials for application in energy-efficient buildings, in: F. Pacheco-Torgal, C.-G. Granqvist, B.P. Jelle, G.P. Vanoli, N. Bianco, J. Kurnitski (Eds.), Cost-Effective Energy Efficient Building Retrofitting, Woodhead Publishing, 2017, pp. 57–118, http://dx.doi.org/10.1016/B978-0-08-101128-7.00003-4, URL https://www.sciencedirect.com/science/article/pii/B9780081011287000034.
[10] O.J. Imafidon, D.S.-K. Ting, Energy consumption of a building with phase change material walls – the effect of phase change material properties, J. Energy Storage 52 (2022) 105080, http://dx.doi.org/10.1016/j.est.2022.105080, URL https://www.sciencedirect.com/science/article/pii/S2352152X22010829.
[11] J. Quesada Allerhand, O. Berk Kazanci, B.W. Olesen, Energy and thermal comfort performance evaluation of PCM ceiling panels for cooling a renovated office room, E3S Web Conf. 111 (2019) 03020, http://dx.doi.org/10.1051/e3sconf/201911103020.
[12] A. Madad, T. Mouhib, A. Mouhsen, Phase change materials for building applications: A thorough review and new perspectives, Buildings 8 (5) (2018) http://dx.doi.org/10.3390/buildings8050063, URL https://www.mdpi.com/2075-5309/8/5/63.
[13] A.R. Abdulmunem, P.M. Samin, K. Sopian, S. Hoseinzadeh, H.A. Al-Jaber, D.A. Garcia, Waste chicken feathers integrated with phase change materials as new inner insulation envelope for buildings, J. Energy Storage 56 (2022) 106130, http://dx.doi.org/10.1016/j.est.2022.106130, URL https://www.sciencedirect.com/science/article/pii/S2352152X22021181.
[14] A.R. Abdulmunem, N.F. Hussein, P.M. Samin, K. Sopian, H.A. Hussien, H. Ghazali, Integration of recycled waste paper with phase change material in building enclosure, J. Energy Storage 64 (2023) 107140, http://dx.doi.org/10.1016/j.est.2023.107140, URL https://www.sciencedirect.com/science/article/pii/S2352152X23005376.
[15] S. Rucevskis, P. Akishin, A. Korjakins, Performance evaluation of an active PCM thermal energy storage system for space cooling in residential buildings, Environ. Climate Technol. 23 (2) (2019) 74–89, http://dx.doi.org/10.2478/rtuect-2019-0056.
[16] L.F. Nielsen, E. Bourdakis, O.B. Kazanci, B.W. Olesen, The influence of a radiant panel system with integrated phase change material on energy use and thermal indoor environment, in: Proceedings of the ASHRAE Winter Conference, 2018.
[17] A. Gallardo, U. Berardi, Analysis of the energy and thermal performance of a radiant cooling panel system with integrated phase change materials in very hot and humid conditions, 609, 2019, 052025, http://dx.doi.org/10.1088/1757-899x/609/5/052025.
[18] C. Stefansen, H. Farhan, E. Bourdakis, O.B. Kazanci, B.W. Olesen, Simulation study of performance of active ceilings with phase change material in office buildings under extreme climate conditions, in: ASHRAE 2018 Winter Conference, American Society of Heating, Refrigerating and Air-Conditioning Engineers, 2018.
[19] D.-I. Bogatu, O.B. Kazanci, B.W. Olesen, An experimental study of the active cooling performance of a novel radiant ceiling panel containing phase change material (PCM), Energy Build. 243 (2021) 110981, http://dx.doi.org/10.1016/j.enbuild.2021.110981, URL https://www.sciencedirect.com/science/article/pii/S0378778821002656.
[20] D.-I. Bogatu, E. Bourdakis, O.B. Kazanci, B.W. Olesen, Experimental comparison of radiant ceiling panels and ceiling panels containing phase change material (PCM), E3S Web Conf. 111 (2019) 01072, http://dx.doi.org/10.1051/e3sconf/201911101072.
[21] H. Weinläder, F. Klinker, M. Yasin, PCM cooling ceilings in the energy efficiency center—passive cooling potential of two different system designs, Energy Build. 119 (2016) 93–100, http://dx.doi.org/10.1016/j.enbuild.2016.03.031, URL https://www.sciencedirect.com/science/article/pii/S0378778816301682.
[22] H. Weinläder, F. Klinker, M. Yasin, PCM cooling ceilings in the energy efficiency center – regeneration behaviour of two different system designs, Energy Build. 156 (2017) 70–77, http://dx.doi.org/10.1016/j.enbuild.2017.09.010, URL https://www.sciencedirect.com/science/article/pii/S0378778817321540.
[23] J. Skovajsa, P. Drabek, S. Sehnalek, M. Zalesak, Design and experimental evaluation of phase change material based cooling ceiling system, Appl. Therm. Eng. 205 (2022) 118011, http://dx.doi.org/10.1016/j.applthermaleng.2021.118011, URL https://www.sciencedirect.com/science/article/pii/S1359431121014319.
[24] B. Nie, Z. Du, B. Zou, Y. Li, Y. Ding, Performance enhancement of a phase-change-material based thermal energy storage device for air-conditioning applications, Energy Build. 214 (2020) 109895, http://dx.doi.org/10.1016/j.enbuild.2020.109895, URL https://www.sciencedirect.com/science/article/pii/S0378778819325940.

[25] T. Korth, F. Loistl, A. Storch, R. Schex, A. Krönauer, C. Schweigler, Capacity enhancement of air conditioning systems by direct integration of a latent heat storage unit, Appl. Therm. Eng. 167 (2020) 114727, http://dx.doi.org/10.1016/j.applthermaleng.2019.114727, URL https://www.sciencedirect.com/science/article/pii/S1359431119319672.

[26] A. Gallardo, U. Berardi, Design and control of radiant ceiling panels incorporating phase change materials for cooling applications, Appl. Energy 304 (2021) 117736, http://dx.doi.org/10.1016/j.apenergy.2021.117736, URL https://www.sciencedirect.com/science/article/pii/S0306261921010837.

[27] Y.-K. Kang, H. Lim, S.-Y. Cheon, J.-W. Jeong, Phase-change material-integrated thermoelectric radiant panel: Experimental performance analysis and system design, Appl. Therm. Eng. 194 (2021) 117082, http://dx.doi.org/10.1016/j.applthermaleng.2021.117082, URL https://www.sciencedirect.com/science/article/pii/S1359431121005251.

[28] S. Mousavi, B. Rismanchi, S. Brey, L. Aye, Thermal and energy performance evaluation of a full-scale test cabin equipped with PCM embedded radiant chilled ceiling, Build. Environ. 237 (2023) 110348, http://dx.doi.org/10.1016/j.buildenv.2023.110348, URL https://www.sciencedirect.com/science/article/pii/S036013232300375X.

[29] M. Andrés-Chicote, A. Tejero-González, E. Velasco-Gómez, F.J. Rey-Martínez, Experimental study on the cooling capacity of a radiant cooled ceiling system, Energy Build. 54 (2012) 207–214, http://dx.doi.org/10.1016/j.enbuild.2012.07.043, URL https://www.sciencedirect.com/science/article/pii/S0378778812003982.

[30] J. Gilbert, U. Koster, PCM Guidebook, DuPont™ Energain®, 2010.

[31] S. Guichard, F. Miranville, D. Bigot, B. Malet-Damour, H. Boyer, Experimental investigation on a complex roof incorporating phase-change material, Energy Build. 108 (2015) 36–43, http://dx.doi.org/10.1016/j.enbuild.2015.08.055.

[32] Ventilation for buildings - chilled ceilings - testing and rating, Standards, Office for Standards, Metrology and Testing, Praha, 2004.

[33] Ergonomics of the thermal environment - analytical determination and interpretation of thermal comfort using calculation of the PMV and ppd indices and local thermal comfort criteria, Standards, Office for Standards, Metrology and Testing, Praha, 2006.

[34] Thermal protection of buildings - part 2: Requirements, Standards, Office for Standards, Metrology and Testing, Praha, 2011.

[35] Energy performance of buildings - energy needs for heating and cooling, internal temperatures and sensible and latent heat loads - part 1: Calculation procedures, Standards, Office for Standards, Metrology and Testing, Praha, 2019.

[36] Energy performance of buildings - ventilation for buildings - part 1: Indoor environmental input parameters for design and assessment of energy performance of buildings addressing indoor air quality, thermal environment, lighting and acoustics - module M1-6, Standards, Office for Standards, Metrology and Testing, Praha, 2020.

[37] M.S. Shin, K.N. Rhee, S.H. Park, M.S. Yeo, K.W. Kim, Enhancement of cooling capacity through open-type installation of cooling radiant ceiling panel systems, Build. Environ. 148 (2019) 417–432, http://dx.doi.org/10.1016/j.buildenv.2018.11.005, URL https://www.sciencedirect.com/science/article/pii/S0360132318307005.

[38] A. Takudzwa Muzhanje, M. Hassan, H. Hassan, Phase change material based thermal energy storage applications for air conditioning: Review, Appl. Therm. Eng. 214 (2022) 118832, http://dx.doi.org/10.1016/j.applthermaleng.2022.118832, URL https://www.sciencedirect.com/science/article/pii/S1359431122007724.

[39] G. Gholamibozanjani, M. Farid, Application of an active PCM storage system into a building for heating/cooling load reduction, Energy 210 (2020) 118572, http://dx.doi.org/10.1016/j.energy.2020.118572, URL https://www.sciencedirect.com/science/article/pii/S0360544220316807.